AD-A071 006 MASSACHUSETTS INST OF TECH LEXINGTON LINCOLN LAB F/G 20/6
ATMOSPHERIC EXTINCTION. I. SYNTHETIC DATA.(U)
APR 79 J M SORVARI F19628-78-C-0002
UNCLASSIFIED EST-43 ESD-TR-79-75 NL

| OF |
AD
A071 006

END
DATE
FILMED
8 -79
DDC

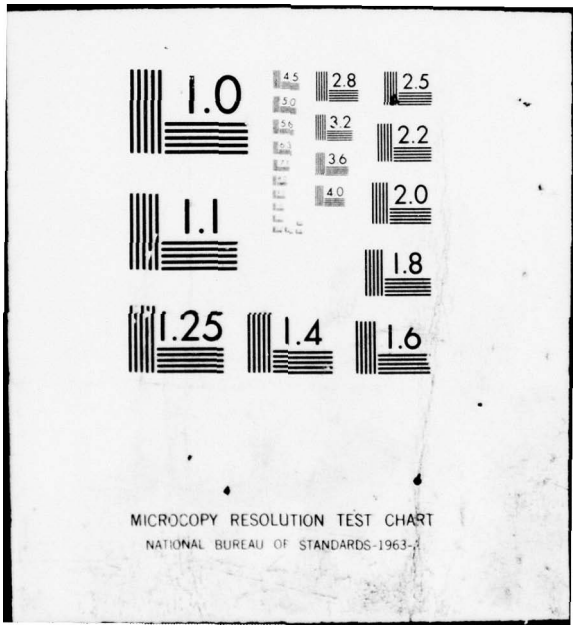
1.0
1.1
1.25
1.4
1.6
1.8
2.0
2.2
2.5
2.8
3.2
3.6
4.0
4.5
5.0
5.6
6.3
7.1
MICROCOPY RESOLUTION TEST CHART
NATIONAL BUREAU OF STANDARDS-1963-A

LEVEL

Project Report

ETS-43

J. M. Sorvari

Atmospheric Extinction, I. Synthetic Data

12 April 1979

Prepared for the Department of the Air Force
under Electronic Systems Division Contract F19628-78-C-0002 by

Lincoln Laboratory
MASSACHUSETTS INSTITUTE OF TECHNOLOGY
LEXINGTON, MASSACHUSETTS

The work reported in this document was performed at Lincoln Laboratory, a center for research operated by Massachusetts Institute of Technology, with the support of the Department of the Air Force under Contract F19628-78-C-0002.

This technical report has been reviewed and is approved for publication.

FOR THE COMMANDER

Joseph C. Sytek
Project Officer
Lincoln Laboratory Project Office

MASSACHUSETTS INSTITUTE OF TECHNOLOGY

LINCOLN LABORATORY

ATMOSPHERIC EXTINCTION, I. SYNTHETIC DATA

J. M. SORVARI

Group 94

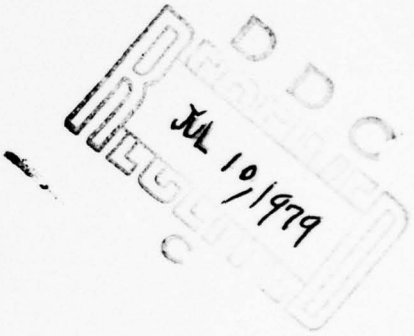

PROJECT REPORT ETS-43

12 APRIL 1979

LEXINGTON MASSACHUSETTS

ABSTRACT

Synthetic data, simulating the effects of atmospheric extinction on GEODSS observations, are presented. Approximate representations for the atmospheric extinction coefficients and for spectral photon distributions are also developed. Together these data are intended for evaluation of the effects of the atmosphere on SOI data, and for the development and testing of models for correcting atmospheric extinction.

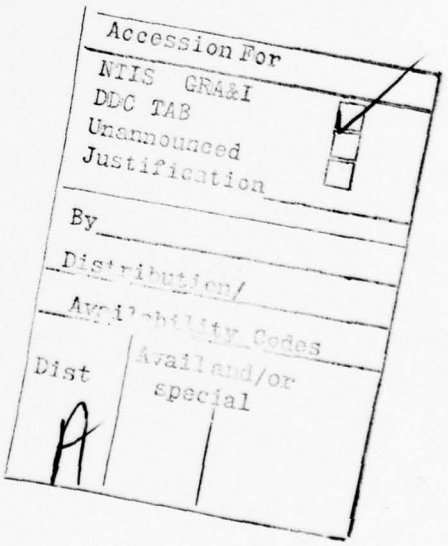

CONTENTS

I. INTRODUCTION

The correction of astronomical brightness measurements for the effects of atmospheric extinction is a complicated process for which no universally satisfactory procedure exists. The problem is especially difficult in the case of the establishment of a catalog of reference standards. Here, mediocre extinction corrections can lead tc unacceptably large systematic errors which destroy the internal consistency of the catalog. The problem has been extensively studied for the conditions appropriate to typical astronomical measurements. The conditions of GEODSS measurements, however, are rather different and the appropriate methodology for these corrections is not well developed. See references (1) and (2) for discussions of the fundamental correction process.

There are two approaches to making extinction corrections: direct integration and modeling. If the spectral distribution, $I(\lambda)$, of the source being measured and the monochromatic extinction coefficient, $k(\lambda)$, are known then a broadband extinction may be calculated by direct integration. If $I(\lambda)$ and $k(\lambda)$ are among the unknowns sought, an iterative technique can be expected to converge given enough data. Unfortunately, the amount of data required for this to work rules it out in the case of GEODSS and even most astronomical observations. Modeling works by finding useful (*i.e.*, some tradeoff between accurate and simple) approximations to such quantities as $k(\lambda)$ and developing programs

specifically designed to determine the parameters needed to make extinction corrections. The GEODSS program needs two rather different extinction models. One must be highly precise and need not be particularly simple, the second must be capable of being evaluated using very little observing time and can tolerate relatively poorer precision.

This paper has been prepared in order to facilitate development of extinction correction models for GEODSS photometry. Section II contains values of broadband extinction calculated by direct integration. These are the values that any proposed extinction model must be capable of producing. The model must also work in the other direction and be able to provide the relevant parameters on the basis of observational data contaminated with noise. To test this ability a set of synthetic data has been included. Section III presents approximate functional representations of the relevant physical quantities. These provide the form and initial estimates needed in the development of our extinction model. Finally, the data presented here should prove useful in the evaluation of error budgets for an operating system.

II. SYNTHETIC OBSERVATIONS

The measured magnitude of an object is given by

$$m'_j = m_{oj} + \delta(A;j) + \varepsilon$$

where m'_j = measured magnitude through filter j

m_{oj} = exo-atmospheric (catalog), j-filter magnitude

$\delta(A;j)$ = atmospheric extinction for the j-filter magnitude as a function of airmass, A

ε = error - assumed to be drawn from normal distribution

In order to create a set of m'_j it is first necessary to calculate values of $\delta(A;j)$ and to generate a set of random errors. The δ may be calculated from

$$\delta(A;j) = -\frac{1}{q}\ln\left[\frac{\int I(\lambda)T(A,\lambda)R_j(\lambda)d\lambda}{\int I(d)R_j(\lambda)d\lambda}\right]$$

where $I(\lambda)$ = the spectral distribution of the object

$T(A,\lambda)$ = the atmospheric transmission as a function of wavelength and airmass; $T(A,\lambda) = e^{-qAk(\lambda)}$

A = the airmass, a function of zenith distance

$k(\lambda)$ = the extinction coefficient, in magnitudes, as a function of wavelength

$R_j(\lambda)$ = the instrumental response profile for filter j

q = .4 ln 10

The integrals may be evaluated numerically for known $I(\lambda)$.

TABLE I

WAVELENGTH DEPENDENCE OF ATMOSPHERIC EXTINCTION, SYSTEM RESPONSE, AND PHOTON FLUX FOR SUNLIGHT, SUNLIGHT REFLECTED FROM GOLD, AND BLACK BODY RADIATION AT T = 4400°K, 5800°K, and 6900°K.

λ(μ)	k(λ)	R_E	$R_{E'}$	R_W	R_X	I_{Sun}	I_{Gold}	B44	B58	B69
.30	"∞"	1.00	0.00	0.00	0.00	1.6	0.6	.098	.281	.472
1	2.79	1.00	.00	.00	.00	2.0	0.7	.123	.321	.518
2	2.14	.99	.00	.00	.00	2.4	0.8	.150	.363	.563
3	1.51	.98	.00	.03	.00	2.8	0.9	.181	.406	.606
4	1.19	.97	.00	.13	.00	3.1	1.0	.215	.450	.648
5	1.08	.96	.00	.19	.00	3.3	1.1	.252	.494	.688
6	.96	.95	.00	.29	.00	3.6	1.2	.292	.537	.726
7	.88	.93	.00	.37	.00	4.0	1.3	.335	.580	.761
8	.81	.91	.00	.42	.00	3.8	1.3	.380	.622	.794
9	.75	.91	.00	.44	.00	4.1	1.4	.427	.663	.824
.40	.71	.90	.00	.46	.00	5.7	1.9	.475	.703	.852
1	.67	.88	.00	.47	.00	6.9	2.3	.526	.741	.877
2	.62	.86	.00	.48	.00	7.2	2.5	.577	.777	.900
3	.59	.84	.01	.47	.00	7.2	2.5	.630	.812	.920
4	.54	.82	.30	.47	.00	8.0	2.9	.683	.845	.938
5	.51	.80	.59	.46	.00	9.0	3.3	.736	.876	.953
6	.48	.79	.63	.45	.00	9.2	3.6	.790	.905	.967
7	.45	.77	.65	.39	.00	9.3	3.8	.843	.931	.978
8	.44	.76	.66	.33	.00	9.4	4.1	.896	.956	.987
9	.41	.75	.66	.35	.00	9.6	4.5	.949	.979	.994

TABLE I (Continued)

λ(μ)	k(λ)	R_E	$R_{E'}$	R_W	R_X	I_{Sun}	I_{Gold}	B44	B109	B69
.50	.40	.74	.65	.19	.00	9.8	5.0	1.000	1.000	1.000
1	.39	.73	.64	.13	.00	9.9	6.3	1.050	1.019	1.004
2	.38	.71	.63	.09	.00	10.0	6.9	1.100	1.036	1.006
3	.36	.70	.62	.07	.00	10.1	7.3	1.148	1.051	1.007
4	.35	.69	.61	.05	.00	10.2	7.7	1.194	1.065	1.007
5	.34	.68	.60	.05	.00	10.3	7.9	1.239	1.077	1.005
6	.33	.67	.59	.04	.00	10.3	8.0	1.283	1.087	1.002
7	.33	.66	.58	.03	.01	10.4	8.3	1.324	1.095	0.999
8	.32	.65	.57	.02	.03	10.4	8.4	1.364	1.103	.994
9	.31	.65	.57	.01	.13	10.5	8.7	1.402	1.108	.988
.60	.31	.64	.56	.01	.31	10.6	8.9	1.438	1.113	.982
1	.30	.63	.56	.01	.37	10.5	8.9	1.473	1.116	.975
2	.29	.62	.55	.01	.41	10.5	9.0	1.505	1.118	.967
3	.27	.62	.55	.00	.39	10.4	9.0	1.536	1.118	.959
4	.25	.61	.54	.00	.37	10.4	9.2	1.565	1.118	.950
5	.24	.60	.53	.00	.35	10.3	9.2	1.592	1.117	.940
6	.23	.59	.53	.00	.34	10.3	9.3	1.617	1.115	.931
7	.22	.58	.52	.00	.31	10.3	9.4	1.640	1.112	.921
8	.22	.57	.51	.00	.28	10.2	9.4	1.662	1.108	.910
9	.21	.57	.51	.00	.25	10.2	9.4	1.682	1.104	.900
.70	.21	.56	.51	.00	.23	10.2	9.5	1.700	1.098	.889
1	.21	.56	.50	.00	.21	10.1	9.4	1.717	1.093	.878
2	.20	.55	.50	.00	.19	10.0	9.4	1.732	1.086	.867
3	.19	.55	.50	.00	.16	9.9	9.3	1.745	1.079	.855
4	.20	.54	.49	.00	.14	9.8	9.2	1.757	1.072	.844

TABLE I (Continued)

$\lambda(\mu)$	$k(\lambda)$	R_E	$R_{E'}$	R_W	R_X	I_{Sun}	I_{Gold}	B44	B58	B69
.75	.21	.54	.49	.00	.12	9.7	9.1	1.767	1.064	.833
6	.57	.53	.48	.00	.11	9.7	9.1	1.777	1.056	.821
7	.19	.53	.48	.00	.09	9.6	9.1	1.784	1.047	.809
8	.17	.52	.47	.00	.08	9.5	9.0	1.791	1.038	.798
9	.16	.52	.47	.00	.06	9.4	8.9	1.796	1.029	.786
.80	.15	.51	.46	.00	.05	9.3	8.8	1.800	1.020	.775
1	.16	.51	.46	.00	.04	9.2	8.7	1.803	1.010	.763
2	.18	.50	.46	.00	.04	9.1	8.6	1.805	1.000	.752
3	.22	.49	.45	.00	.03	9.0	8.6	1.806	.990	.741
4	.18	.48	.44	.00	.02	8.9	8.5	1.806	.980	.729
5	.16	.46	.42	.00	.01	8.8	8.4	1.805	.969	.718
6	.15	.44	.40	.00	.01	8.7	8.4	1.803	.959	.707
7	.14	.40	.36	.00	.00	8.6	8.3	1.800	.948	.696
8	.19	.35	.32	.00	.00	8.5	8.2	1.797	.938	.685
9	.27	.28	.25	.00	.00	8.4	8.1	1.793	.927	.675
.90	.31	.21	.19	.00	.00	8.3	8.0	1.788	.916	.664
1	.34	.14	.13	.00	.00	8.2	7.9	1.782	.905	.654
2	.54	.02	.02	.00	.00	8.1	7.8	1.776	.895	.643
3	.64	.01	.01	.00	.00	8.1	7.8	1.769	.884	.633
4	.55	.00	.00	.00	.00	8.0	7.7	1.761	.873	.623

The values needed to carry out the integrations are tabulated as Table I. R_E and $R_{E'}$ are the unfiltered GaAs photocathode response and the GaAs response modified by the addition of a Schott GG435 filter. This modification was made in an attempt to make the extinction characteristics more tractable. R_W and R_X are the effective profiles of the W- and X-filters of the Lincoln three-color system. These are defined by 1mm BG18 plus 1mm BG27 for W and 3mm OG590 plus 2mm KG3 for X, with a GaAs photocathode. The central wavelength and full width at half power are respectively 4300Å and 1400Å, and 6720Å and 1200Å. Five spectral distributions are listed: sunlight, sunlight reflected from gold, and black body radiation at 4400°K, 5800°K, and 6900°K. These temperatures correspond to the effective temperatures of stars of spectral types K2, G2, and F2, *i.e.*, the sun's type and one type to either side. The atmospheric extinction coefficients are for a "typical" atmosphere as described in appendix B of reference (3).

Values of the ratio

$$\frac{\int I(\lambda) R_j(\lambda) T(A,\lambda) d\lambda}{\int I(\lambda) R_j(d) d\lambda}$$

were calculated for several values of the air mass and for all combinations of $I(\lambda)$ and $R_j(\lambda)$. These values were converted into astronomical magnitudes and are tabulated as Table II. The first section of the table lists values of the atmospheric extinction

TABLE II

VALUES OF THE ATMOSPHERIC EXTINCTION AS A FUNCTION OF AIR MASS FOR A VARIETY OF SOURCE SPECTRAL DISTRIBUTIONS. For sunlight, the column labeled X' contains values calculated with the "extra" extinction at $\lambda = .76\mu$ removed.

a. SUNLIGHT

Air Mass	E	E'	W	X	X'
1.0	$0^m.372$	$0^m.288$	$0^m.555$	$0^m.252$	$0^m.238$
1.25	.456	.358	.690	.315	.297
1.5	.538	.428	.824	.377	.356
1.75	.617	.497	.956	.439	.415
2.0	.695	.565	1.088	.500	.474
2.5	.847	.701	1.347	.622	.591
3.0	.993	.834	1.601	.744	.708
3.5	1.135	.965	1.852	.864	.825

b. SUNLIGHT - GOLD

	E	E'	W	X
1.0	$0^m.309$	$0^m.268$	$0^m.524$	$0^m.251$
1.25	.381	.334	.652	.313
1.5	.451	.399	.778	.375
1.75	.521	.464	.903	.436
2.0	.589	.528	1.027	.498
2.5	.724	.655	1.271	.619
3.0	.855	.780	1.511	.740
3.5	.983	.903	1.748	.860

TABLE II (Continued)

c. BLACK - BODY 4400°K

Air Mass	E	E'	W	X
1.0	$0^m.315$	$0^m.266$	$0^m.541$	$0^m.250$
1.25	.388	.331	.673	.312
1.5	.460	.395	.804	.373
1.75	.530	.459	.933	.434
2.0	.599	.523	1.061	.495
2.5	.734	.648	1.313	.615
3.0	.865	.772	1.561	.735
3.5	.993	.893	1.805	.854

d. BLACK - BODY 5800°K

	E	E'	W	X
1.0	$0^m.395$	$0^m.286$	$0^m.574$	$0^m.252$
1.25	.482	.356	.714	.314
1.5	.566	.425	.851	.376
1.75	.647	.494	.988	.438
2.0	.727	.562	1.122	.499
2.5	.881	.697	1.388	.621
3.0	1.029	.829	1.649	.742
3.5	1.172	.960	1.905	.863

TABLE II (Continued)

e. BLACK - BODY $6900^{o}K$

Air Mass	E	E'	W	X
1.0	$0^{m}.452$	$0^{m}.295$	$0^{m}.593$	$0^{m}.253$
1.25	.547	.368	.736	.316
1.5	.639	.439	.878	.378
1.75	.727	.510	1.018	.440
2.0	.813	.580	1.157	.502
2.5	.979	.719	1.429	.625
3.0	1.137	.856	1.696	.746
3.5	1.289	.990	1.958	.867

for sunlight as seen by the four response profiles R_E, $R_{E'}$, R_W, and R_X, and an additional column labled X'. This column contains values of extinction arising from a modified atmospheric extinction - one having the "extra" extinction due to the atmospheric A-band removed. This has been done to facilitate later comparison with a simple model which does not include the effect of the A-band. Two effects of the wavelength dependence of atmospheric extinction are immediately evident. First, the extinction in the bluest filter (W) is much the highest, and second, for any response bluer objects (here, black body radiation at higher T) suffer greater extinction.

Random errors were generated in the following way. A pseudo-random number generator was programmed to provide numbers evenly distributed over the interval $-.5 \leq y \leq +.5$. A value of t was found such that $|y| = (2\pi)^{-\frac{1}{2}} \int_o^t e^{-x^2/2} dx$, and the sign of y was then assigned to t. The numbers t are thus drawn from a normal distribution with a mean of zero and standard deviation of unity. In fact, for the values of t used, $\bar{t} = -0.007$ and $\sigma = 1.059$. Values of t were then multiplied by a typical mean error of a single observation and added to the magnitude to produce the synthetic data. Two typical values were used, a constant $0^m.030$ and an air mass proportional $0^m.010\ A^2$.

Synthetic data were generated for ten "objects": two blackbody sources at each temperature, three sunlight sources, and a sunlight from gold source. Instead of using the two magnitudes

TABLE III

CATALOG MAGNITUDES FOR OBJECTS FOR
WHICH SYNTHETIC OBSERVATIONS WERE GENERATED

OBJ	$m_{e,x\,o}$	C_o	REMARKS
1	6.300	$0^m.715$	BB, T = 4400°K
2	7.250	0.715	BB, T = 4400°K
3	4.650	0.064	BB, T = 5800°K
4	5.900	0.064	BB, T = 5800°K
5	5.550	-0.269	BB, T = 6900°K
6	6.850	-0.269	BB, T = 6900°K
7	5.800	0.101	Sunlight
8	6.350	0.101	Sunlight
9	7.150	0.101	Sunlight
10	6.000	0.944	Sunlight reflected from gold

m_w and m_x, the usual practice of using a magnitude, m_x, and a color, $C \equiv m_w - m_x$, has been followed. For simplicity the X-magnitude and the E-magnitudes are taken to be equal. The catalog values for these ten objects are listed in Table III. The synthesized observations are listed in Table IV. Data are organized into three "runs" for each object. Runs 1 and 2 use an irregular selection of five values of airmass spanning the range of values calculated. Runs 3 all use the same regular series of six airmasses. For runs 1, the constant standard deviation error was added, while for runs 2 and 3 the airmass proportional error was applied.

TABLE IV

SYNTHETIC OBSERVATIONS OF TEN OBJECTS

Obj	Run	A	M'_E	$M'_{E'}$	M'_x	C'
1	1	1.0	6.66	6.56	6.54	1.02
		1.25	6.71	6.64	6.57	1.08
		2.0	6.97	6.87	6.83	1.25
		3.0	7.15	7.09	7.01	1.54
		3.0	7.15	7.02	7.05	1.53
	2	1.25	6.70	6.64	6.63	1.10
		1.5	6.74	6.70	6.67	1.13
		2.0	6.88	6.83	6.81	1.26
		2.5	7.05	7.00	6.94	1.38
		3.0	7.19	7.02	7.10	1.41
	3	1.0	6.62	6.57	6.56	1.00
		1.5	7.74	6.72	6.65	1.10
		2.0	6.91	6.83	6.89	1.28
		2.5	7.05	6.83	6.90	1.57
		3.0	7.04	7.10	6.94	1.51
		3.5	7.48	7.11	7.21	1.66

Obj	Run	A	M'_E	$M'_{E'}$	M'_x	C'
2	1	1.25	7.65	7.61	7.52	1.10
		1.25	7.61	7.54	7.55	1.11
		2.0	7.83	7.82	7.72	1.28
		3.0	8.09	8.00	8.00	1.52
		3.5	8.25	8.16	8.13	1.67
	2	1.0	7.56	7.50	7.50	1.01
		1.25	7.64	7.60	7.56	1.06
		1.75	7.72	7.78	7.67	1.17
		3.0	8.09	7.98	7.92	1.58
		3.0	8.12	8.07	8.02	1.49
	3	1.0	7.58	7.52	7.50	1.02
		1.5	7.67	7.64	7.60	1.15
		2.0	7.89	7.79	7.71	1.26
		2.5	7.92	7.78	7.84	1.44
		3.0	8.10	8.12	8.28	1.45
		3.5	8.10	8.12	8.13	1.95

TABLE IV (Continued)

Obj	Run	A	M'_E	$M'_{E'}$	M'_x	C'
3	1	1.25	5.08	5.00	4.91	0.50
		1.5	5.20	5.03	4.99	.51
		2.0	5.37	5.22	5.15	.68
		3.0	5.66	5.53	5.38	.95
		3.5	5.81	5.62	5.52	1.07
	2	1.25	5.14	5.03	4.93	.45
		1.25	5.12	5.02	4.97	.47
		1.75	5.33	5.16	5.10	.58
		3.0	5.74	5.35	5.33	1.13
		3.5	5.71	5.50	5.49	.97
	3	1.0	5.04	4.92	4.91	.37
		1.5	5.22	5.05	5.07	.53
		2.0	5.43	5.28	5.09	.81
		2.5	5.50	5.42	5.24	.87
		3.0	5.73	5.49	5.43	.93
		3.5	5.91	5.66	5.51	1.07
4	1	1.0	6.26	6.18	6.16	0.39
		1.5	6.48	6.34	6.26	.52
		2.5	6.83	6.59	6.54	.84
		3.5	7.06	6.89	6.78	1.10
		3.5	7.02	6.90	6.80	1.09
	2	1.0	6.28	6.18	6.14	.38
		1.25	6.36	6.27	6.24	.43
		1.75	6.60	6.44	6.32	.66
		3.0	6.88	6.93	6.71	.96
		3.0	6.86	6.54	6.60	1.17
	3	1.0	6.30	6.19	6.14	.39
		1.5	6.44	6.30	6.29	.51
		2.0	6.63	6.42	6.37	.75
		2.5	6.71	6.48	6.62	.83
		3.0	6.90	6.86	6.68	1.00
		3.5	6.79	6.80	6.54	1.29

TABLE IV (Continued)

Obj	Run	A	M'_E	$M'_{E'}$	M'_x	C'
5	1	1.0	5.97	5.88	5.78	0.04
		1.25	6.13	5.94	5.86	.19
		2.0	6.36	6.11	6.06	.40
		3.0	6.67	6.41	6.32	.68
		3.0	6.71	6.41	6.30	.63
	2	1.25	6.13	5.92	5.85	.15
		1.5	6.26	6.02	5.93	.25
		1.75	6.25	6.04	5.93	.30
		3.0	6.57	6.44	6.28	.63
		3.5	6.96	6.57	6.35	.71
	3	1.0	6.01	5.84	5.79	.08
		1.5	6.17	5.99	5.92	.24
		2.0	6.36	6.15	6.08	.40
		2.5	6.45	6.28	6.16	.42
		3.0	6.64	6.39	6.29	.57
		3.5	6.78	6.61	6.26	.69
6	1	1.0	7.32	7.14	7.12	0.12
		1.5	7.47	7.26	7.26	.25
		2.5	7.85	7.54	7.47	.51
		3.0	7.90	7.70	7.55	.70
		3.0	8.00	7.71	7.58	.69
	2	1.25	7.38	7.23	7.19	.14
		1.25	7.39	7.20	7.19	.13
		1.75	7.60	7.36	7.31	.29
		3.0	7.92	7.63	7.61	.88
		3.5	7.89	7.88	7.86	.71
	3	1.0	7.27	7.15	7.11	.06
		1.5	7.55	7.27	7.22	.22
		2.0	7.70	7.36	7.35	.41
		2.5	7.88	7.52	7.46	.36
		3.0	7.91	7.76	7.66	.92
		3.5	8.00	7.97	7.71	.93

TABLE IV (Continued)

Obj	Run	A	M'_E	$M'_{E'}$	M'_x	C'
7	1	1.0	6.16	6.10	6.10	0.48
		1.25	6.24	6.13	6.11	.45
		1.75	6.44	6.32	6.23	.64
		3.0	6.87	6.60	6.56	.98
		3.5	6.99	6.75	6.69	1.10
	2	1.25	6.23	6.14	6.10	.44
		1.5	6.35	6.22	6.15	.59
		2.0	6.48	6.38	6.23	.72
		3.0	6.73	6.63	6.60	1.06
		3.0	6.74	6.55	6.56	.99
	3	1.0	6.16	6.09	6.06	.40
		1.5	6.30	6.23	6.20	.55
		2.0	6.51	6.49	6.34	.69
		2.5	6.72	6.57	6.30	.79
		3.0	6.81	6.77	6.35	.75
		3.5	6.90	6.84	6.79	1.05

Obj	Run	A	M'_E	$M'_{E'}$	M'_x	C'
8	1	1.25	6.80	6.68	6.65	0.49
		1.5	6.91	6.78	6.77	.53
		1.75	6.98	6.83	6.83	.56
		3.5	7.49	7.33	7.20	1.05
		3.5	7.51	7.31	7.24	1.11
	2	1.0	6.72	6.62	6.61	.41
		1.5	6.86	6.79	6.72	.53
		2.5	7.23	7.08	6.93	.75
		3.0	7.31	7.24	7.13	1.05
		3.5	7.52	7.22	7.28	1.01
	3	1.0	6.75	6.64	6.59	.41
		1.5	6.88	6.77	6.75	.53
		2.0	7.03	6.98	6.82	.73
		2.5	7.12	7.06	6.92	.77
		3.0	7.19	7.22	7.13	.93
		3.5	7.35	7.49	7.16	1.18

TABLE IV (Continued)

Obj	Run	A	M'_E	$M'_{E'}$	M'_x	C'
9	1	1.0	7.56	7.41	7.43	0.42
		1.25	7.64	7.53	7.45	.52
		2.0	7.85	7.71	7.64	.66
		3.0	8.16	7.97	7.90	1.04
		3.5	8.23	8.10	7.98	1.11
	2	1.25	7.60	7.51	7.46	.50
		1.5	7.66	7.57	7.54	.53
		1.75	7.82	7.67	7.56	.67
		3.0	8.05	8.10	7.98	.83
		3.0	8.24	8.06	7.92	.84
	3	1.0	7.52	7.42	7.39	.42
		1.5	7.69	7.56	7.58	.54
		2.0	7.84	7.75	7.63	.73
		2.5	8.02	7.91	7.73	87
		3.0	8.17	7.94	7.84	1.22
		3.5	8.29	8.03	8.00	1.07
10	1	1.0	6.36	6.24	6.26	1.22
		1.5	6.52	6.35	6.37	1.30
		2.0	6.60	6.50	6.54	1.48
		3.0	6.84	6.75	6.77	1.77
		3.5	7.02	6.86	6.83	1.86
	2	1.0	6.32	6.26	6.25	1.21
		1.25	6.42	6.36	6.32	1.29
		2.5	6.66	6.66	6.57	1.44
		3.5	6.86	6.81	6.89	1.73
		3.5	6.96	6.86	6.75	1.91
	3	1.0	6.31	6.26	6.23	1.21
		1.5	6.46	6.41	6.39	1.32
		2.0	6.55	6.52	6.51	1.48
		2.5	6.82	6.86	6.70	1.52
		3.0	6.79	6.77	6.89	1.59
		3.5	6.87	6.93	6.75	1.82

III. APPROXIMATE REPRESENTATIONS

It is useful to have functional representations for some of the data in Table I. Presented here are simple functions which approximate the atmospheric extinction coefficient, the solar photon flux, and the black-body photon flux for $T = 5800^{\circ}K$. These representations can be used for such purposes as developing models of extinction and evaluating specific effects of atmospheric extinction on real data.

For the case of the extinction coefficient, simple polynomials of order three or less do a rather poor job of approximating the wavelength dependence. A good fit, however, is obtained from

$$k(\lambda) \simeq 0.096/(\lambda - .26)$$

Figure 1 shows the fit. The A-band ($\lambda = .76\mu$) is, of course, completely missed by this representation. There is precedent for this form; astronomers have long used a simple $1/\lambda$ extinction law in studies of the interstellar medium. Generalizing this gives

$$k(\lambda) \simeq \frac{\alpha}{\lambda - \lambda'} + \beta$$

Varying α, λ', and β should provide a good approximation to a wide range of atmospheric conditions. Treating λ' as a free parameter, however, introduces enormous complications into the analysis. It also seems likely that the origin of the value of λ' lies in microscopic rather than macroscopic processes and would thus not be expected to vary greatly. Therefore, it seems reasonable to set $\lambda' = .26\mu$ and also to expect $\alpha \geq \beta \geq 0$.

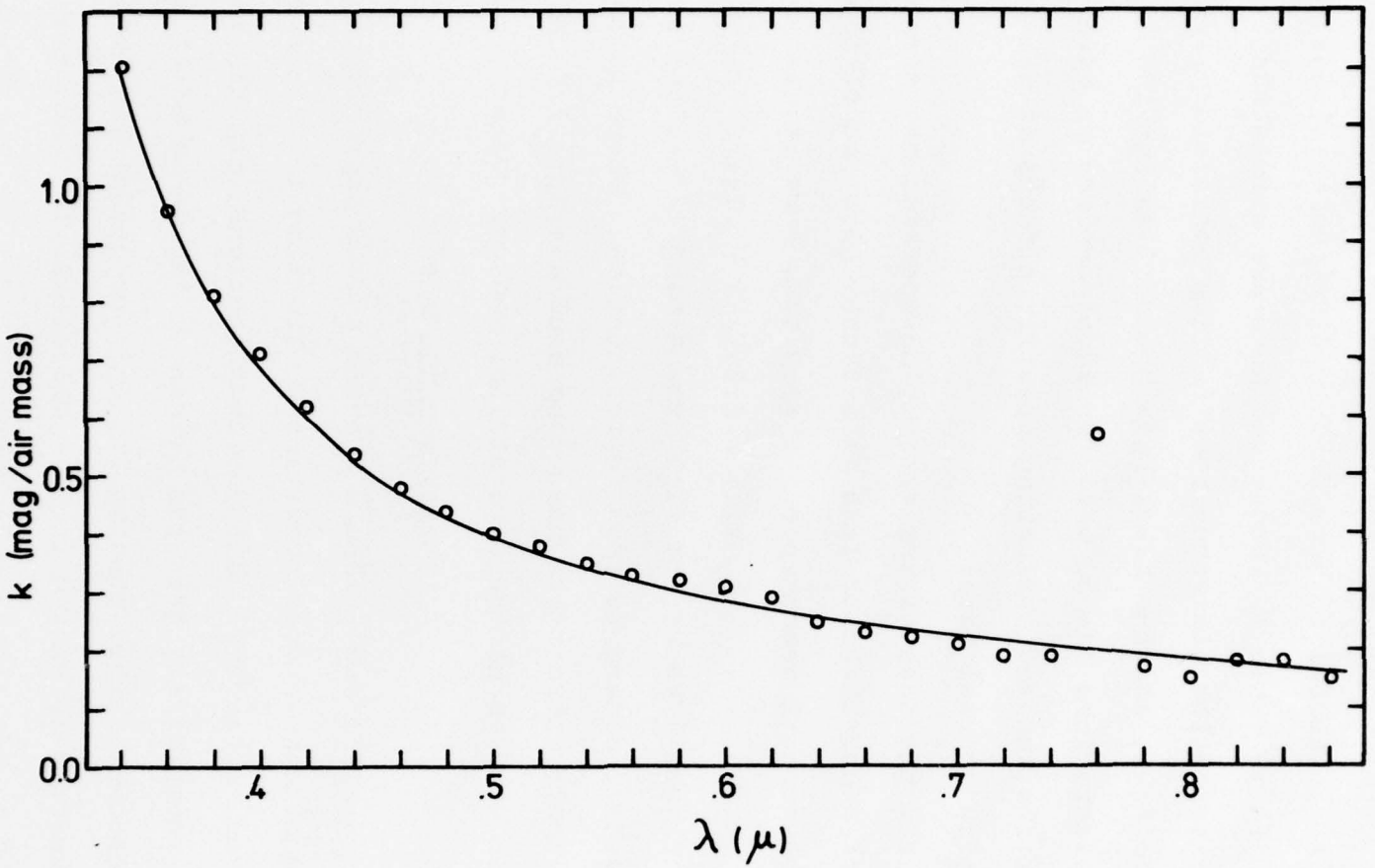

Figure 1. The Atmospheric Extinction Coefficient k(λ). Points are measured values and solid curve is a simple approximation to the continuous extinction.

Using this representation for $k(\lambda)$, it is possible to write a power series expansion for the atmospheric transmission. The transmission law is

$$T(A,\lambda) = e^{-qAK(\lambda)}$$

when $k(\lambda)$ is expressed in astronomical magnitudes per air mass. $T(A,\lambda)$ can be written in the form

$$T(A,\lambda) = T(A,\lambda_o)\left[1 + a_1(A)\left(\frac{\lambda - \lambda_o}{\lambda_o}\right) + a_2(A)\left(\frac{\lambda - \lambda_o}{\lambda_o}\right)^2 + \ldots\right]$$

Evaluating the coefficients gives

$$T(A,\lambda_o) = e^{-qA(K_o + \beta)}$$

$$a_1 = \Lambda_o qAK_o$$

$$a_2 = \tfrac{1}{2}\Lambda_o^2\left[(qA)^2K_o^2 - 2(qA)K_o\right]$$

$$a_3 = \frac{1}{3!}\Lambda_o^3\left[(qA)^3K_o^3 - 6(qA)^2K_o^2 + 6(qA)K_o\right]$$

$$a_4 = \frac{1}{4!}\Lambda_o^4\left[(qA)^4K_o^4 - 12(qA)^3K_o^3 + 36(qA)^2K_o^2 - 24(qA)K_o\right]$$

$$\vdots$$

where

$$\Lambda_o \equiv \frac{\lambda_o}{\lambda_o - .26\mu}$$

$$K_o \equiv \frac{\alpha}{\lambda_o - .26\mu}$$

The solar photon flux may be fairly well approximated by either a cubic polynomial or a black-body distribution. Figure 2 shows measured values of the solar flux compared with a black-body distribution at $T = 5800^{\circ}K$ and the cubic polynomial,

$$I(\lambda) = -53.23(1.00 - 5.12\lambda + 7.11\lambda^2 - 3.18\lambda^3),$$

calculated for the range $.34 \leq \lambda \leq .86$. Note how badly it fails outside this range. It is useful to express the polynomial in powers of $(\lambda - \lambda_o)/\lambda_o$ instead of λ. For $\lambda_o = .55\mu$, for example,

$$I = 10.34\left[1.00 + .52\left(\frac{\lambda - \lambda_o}{\lambda_o}\right) - 2.90\left(\frac{\lambda - \lambda_o}{\lambda_o}\right)^2 + 2.72\left(\frac{\lambda - \lambda_o}{\lambda_o}\right)^3\right]$$

As an additional comparison, a cubic was fit to $T = 5800^{\circ}K$ black-body radiation in the range $.34 \leq \lambda \leq .86$. The function obtained is

$$I = 3.145(1.00 - 5.31\lambda + 6.68\lambda^2 - 2.64\lambda^3)$$

or, again, setting $\lambda_o = .55\mu$

$$I = 1.07\left[1.00 + .58\left(\frac{\lambda - \lambda_o}{\lambda_o}\right) - 2.07\left(\frac{\lambda - \lambda_o}{\lambda_o}\right)^2 + 1.30\left(\frac{\lambda - \lambda_o}{\lambda_o}\right)^3\right]$$

Figure 3 shows this polynomial fit compared to the black-body curve. Again, the cubic deviates from the correct values outside the valid range, although not as badly as in the case of the fit to the other solar flux in Figure 2. Not surprisingly, the coefficients for the black-body fit are similar to those for the solar fit except for the (inconsequential) scaling factor.

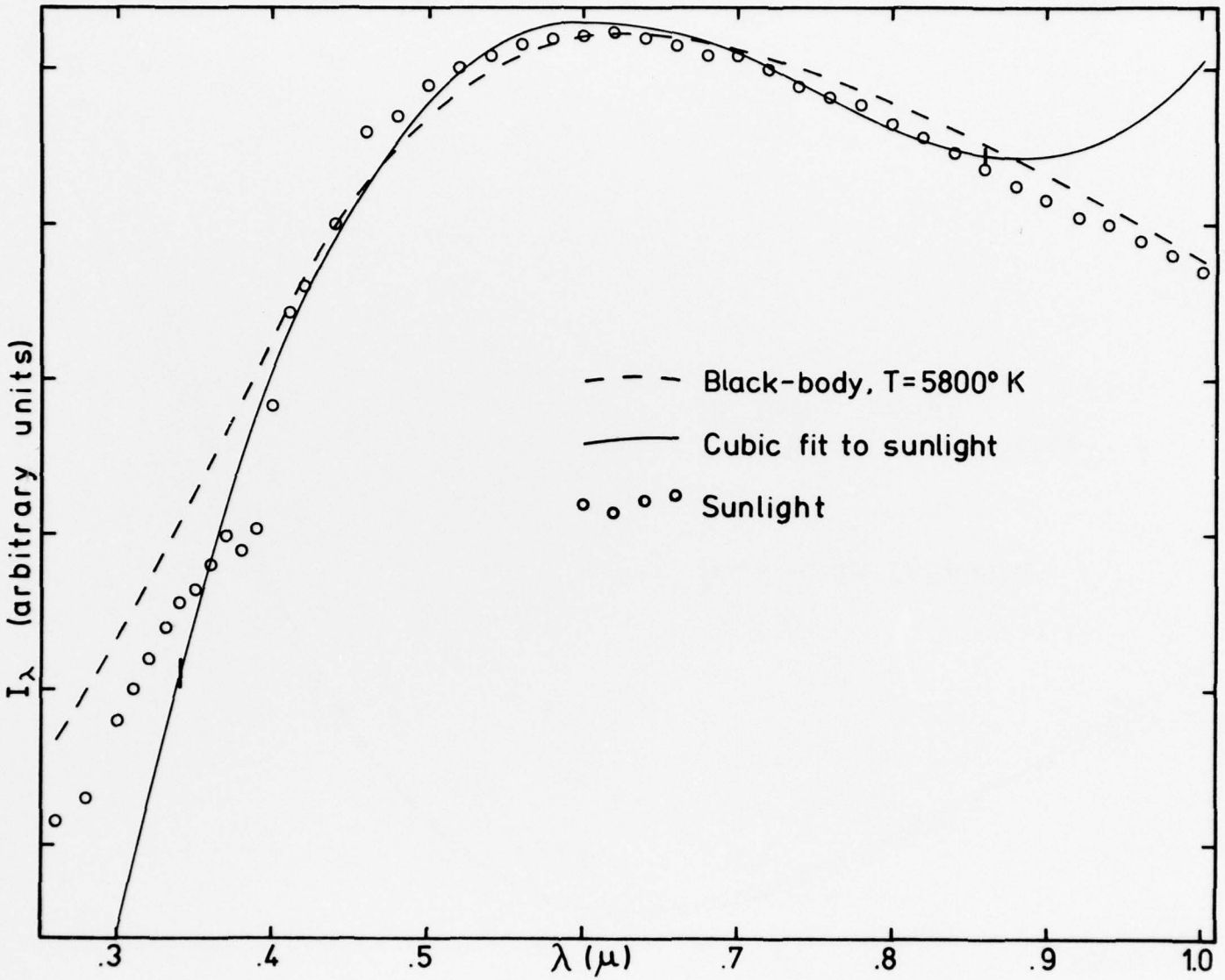

Figure 2. The Solar Photon Flux and Two Approximations.

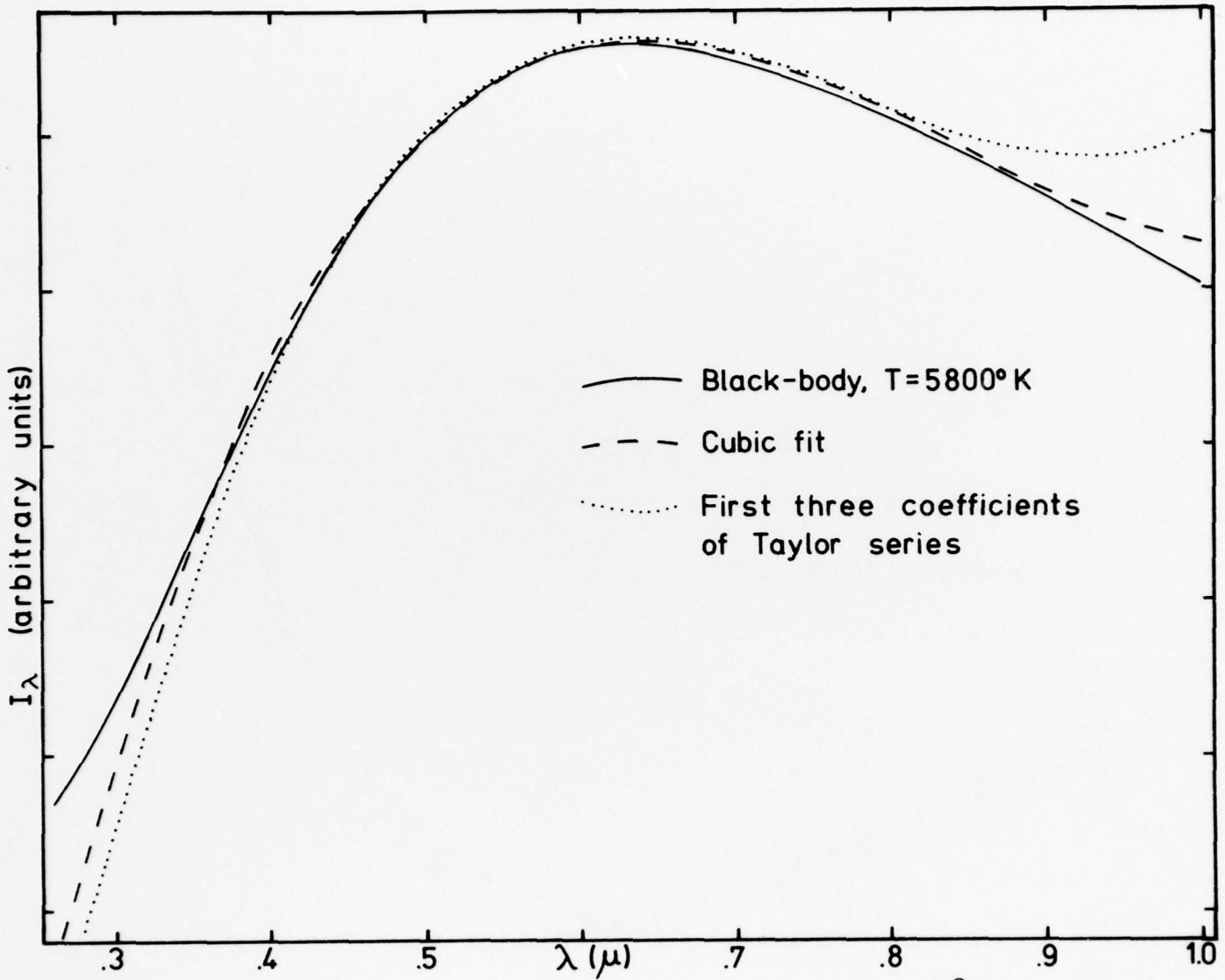

Figure 3. Black-body Radiation at 5800°K.

Finally, the actual black-body functions can be expanded as an infinite order polynomial

$$B(\lambda,T) \sim 1 + b_1(T)\frac{\lambda - \lambda_o}{\lambda_o} + b_2(T)\left(\frac{\lambda - \lambda_o}{\lambda_o}\right)^2 + \ldots$$

Values of the first four coefficients are given in Table VI for $T = 6900^oK$, 5800^oK, and 4400^oK, and for $\lambda_o = .43\mu$, $.55\mu$, and $.67\mu$. The central compartment of Table V, containing the coefficients for $\lambda_o = .55\mu$ and $T = 5800^oK$, should be compared to the coefficients of the cubic polynomial representations.

At this point the meaning and intended use of the expansions for the flux must be examined more carefully. The expansions will generally be used to evaluate integrals in the form

$$\int I(\lambda)f(\lambda)d\lambda = \sum b_n F_n ,$$

where

$$F_n = \int \left(\frac{\lambda - \lambda_o}{\lambda_o}\right)^n f(\lambda)d\lambda$$

The b_n are, of course, just the coefficients in the power series expansion of I,

$$I = \sum_{n}^{\infty} b_n \left(\frac{\lambda - \lambda_o}{\lambda_o}\right)^n$$

and the F_n can be expected to become very small as n increases. Consider now the case of 5800^oK black-body radiation and its two expansions: the cubic fit defined by the three coefficients derived above, and the power series defined by an infinite number of

TABLE V

COEFFICIENTS FOR THE POWER SERIES EXPANSIONS OF THE BLACK-BODY PHOTON DISTRIBUTION.

		λ		
T		.43μ	.55μ	.67μ
4400°K	b_1	3.61	1.96	.92
	b_2	.92	-1.99	-2.41
	b_3	-6.08	-1.80	1.08
	b_4	2.35	4.87	2.19
5800°K	b_1	1.79	.56	- .20
	b_2	-2.14	-2.29	-1.60
	b_3	-1.28	1.83	2.67
	b_4	4.61	0.86	-1.92
6900°K	b_1	.89	- .12	- .74
	b_2	-2.40	-1.70	- .75
	b_3	1.15	2.64	2.41
	b_4	2.08	-1.65	-3.13

coefficients, the first four of which are shown in Table V. Now within the range $.34 \leq \lambda \leq .86$ the three cubic coefficients give a better fit to the data than the first three coefficients from Table V. Nevertheless, a better representation of integrals such as the one shown above would be obtained by using the values from Table V. Thus, even if only the first few coefficients make a significant contribution to the series representation of the integral, they should be evaluated *via* a higher order (ideally, infinite order) fit to the data.

When $I(\lambda)$ is unknown, two additional problems arise. First $I(\lambda)$ will be characterized or characterizable by an intensity and a few color indices. In order to evaluate the integrals, it will be necessary to relate the b_n to these color indices. This leads naturally to the next problem - the non-independence of the b_n. The analysis used to determine $I(\lambda)$ is based on the assumption of independent parameters. When the parameters are not independent the values derived for them will be unreliable. In the case of black-body radiation, there is only one free parameter, T (or equivalently b_1). For real radiation, the strict functional dependence on only one parameter no longer holds, but neither is there a set of many truly independent b_n. It is generally preferable to accept a slightly poorer fit to the data using a minimum of parameters than to improve the fit by adding free parameters of questionable nature.

REFERENCES

1. J. M. Sorvari, "Automatic Sky Quality Assessment I. The Point Measurement Device," Project Report ETS-38, Lincoln Laboratory, M.I.T. (28 November 1978), DDC-AD-A064280.

2. I. King, "Effective extinction values in wide-band photometry". Astron. J., 57, 253 (1952).

3. J. M. Sorvari, "A Photometer for Obtaining SOI Data at the GEODSS ETS," Project Report ETS-37, Lincoln Laboratory, M.I.T. (3 November 1978), DDC-AD-B032502.

UNCLASSIFIED

SECURITY CLASSIFICATION OF THIS PAGE *(When Data Entered)*

REPORT DOCUMENTATION PAGE

READ INSTRUCTIONS BEFORE COMPLETING FORM

1. REPORT NUMBER: ESD-TR-79-75	2. GOVT ACCESSION NO.
3. RECIPIENT'S CATALOG NUMBER	
4. TITLE *(and Subtitle)*: Atmospheric Extinction, I. Synthetic Data	5. TYPE OF REPORT & PERIOD COVERED: Project Report
6. PERFORMING ORG. REPORT NUMBER: Project Report ETS-43	
7. AUTHOR(s): J.M. Sorvari	8. CONTRACT OR GRANT NUMBER(s): F19628-78-C-0002
9. PERFORMING ORGANIZATION NAME AND ADDRESS: Lincoln Laboratory, M.I.T. P.O. Box 73 Lexington, MA 02173	10. PROGRAM ELEMENT, PROJECT, TASK AREA & WORK UNIT NUMBERS: Program Element No. 63428F Project No. 2128
11. CONTROLLING OFFICE NAME AND ADDRESS: Air Force Systems Command, USAF Andrews AFB Washington, DC 20331	12. REPORT DATE: 12 April 1979
	13. NUMBER OF PAGES: 36
14. MONITORING AGENCY NAME & ADDRESS *(if different from Controlling Office)*: Electronic Systems Division Hanscom AFB Bedford, MA 01731	15. SECURITY CLASS. *(of this report)*: Unclassified
	15a. DECLASSIFICATION DOWNGRADING SCHEDULE

16. DISTRIBUTION STATEMENT *(of this Report)*

Approved for public release; distribution unlimited.

17. DISTRIBUTION STATEMENT *(of the abstract entered in Block 20, if different from Report)*

18. SUPPLEMENTARY NOTES

None

19. KEY WORDS *(Continue on reverse side if necessary and identify by block number)*

synthetic data
atmospheric extinction
GEODSS observations
SOI data

20. ABSTRACT *(Continue on reverse side if necessary and identify by block number)*

Synthetic data, simulating the effects of atmospheric extinction on GEODSS observations, are presented. Approximate representations for the atmospheric extinction coefficients and for spectral photon distributions are also developed. Together these data are intended for evaluation of the effects for the atmosphere on SOI data, and for the development and testing of models for correcting atmospheric extinction.

DD FORM 1 JAN 73 1473 EDITION OF 1 NOV 65 IS OBSOLETE

UNCLASSIFIED

SECURITY CLASSIFICATION OF THIS PAGE *(When Data Entered)*

207650